ARTICLE

OBC
www.rsc.org/obc

Excited state tautomerization of azaindole

Michael T. Cash,[a] Peter R. Schreiner[a,b] and Robert S. Phillips[a]

[a] *Department of Chemistry, University of Georgia, Athens, Georgia, 30602, USA. E-mail: prs@chem.uga.edu*

[b] *Justus-Liebig-Universität Giessen, Institut für Organische Chemie, Heinrich-Buff-Ring 58, 35392, Giessen, Germany. E-mail: prs@org.chemie.uni-giessen.de*

Received 12th May 2005, Accepted 10th August 2005
First published as an Advance Article on the web 14th September 2005

Fluorescent tryptophan analogs, like azatryptophan, offer an advantage for exploring protein and peptide structure and dynamics. The chromophoric moieties, azaindole, of the azatryptophan analogs are investigated for their potential as fluorescent probes. The photophysical properties of 4-azaindole (4AI) and 5-azaindole (5AI) and their tautomers are characterized through computational and experimental methods. Both 4AI and 5AI undergo excited state tautomerization in the presence of 1 M NaOH. The protonated forms of 4AI and 5AI have a fluorescence emission of 415 and 410 nm, respectively, while the tautomers of 4AI and 5AI have a fluorescent emission of 480 and 450 nm, respectively. Gas phase computations (B3LYP/6–31+G**) show that the N^1H azaindole tautomer is lower in energy in the ground state by as much as 12.5 kcal mol^{-1}, while the N^nH azaindole tautomer is lower in energy in the excited state by as much as 18.1 kcal mol^{-1}. Solvent effects on the tautomer energy differences were computed using the isodensity polarized continuum model (IPCM). The polarity of the solvent helps to reduce the energy difference between the tautomers in the ground state by as much as 5.8 kcal mol^{-1}, but not enough to reverse the ground state tautomer preference.

Introduction

Tryptophan has been used extensively as an intrinsic fluorescent probe to investigate protein dynamics and structure; tryptophan fluorescence is particularly useful due to its sensitivity to the local environment. A red shift in the fluorescence emission is observed when a tryptophan residue is exposed to solvent relative to a tryptophan buried in a hydrophobic pocket of a protein. In addition, charged amino acid side chains that are in close proximity quench the fluorescence decay of tryptophan, providing additional information about the local environment of the tryptophan residue.[1–5] Several tryptophan analogs with significantly improved fluorescence have been investigated for incorporation into peptides and proteins. The most commonly used analogs include 5-hydroxytryptophan and 7-azatryptophan.[6,8] Each of these analogs offer advantages over natural tryptophan for exploring protein dynamics. The advantages include greater fluorescence intensity, red-shifted fluorescence, and greater sensitivity to the electric field of the local environment.[7]

Ideally, the tryptophan analog incorporated should be structurally similar to natural tryptophan to minimize the potential for perturbation of protein structure and function. The azatryptophan analogs are closer in structure to natural tryptophan than the other analogs bearing hydroxyl and fluoro substituents, which makes azatryptophan ideally suited as an optical spectral probe. In addition, the incorporation of azatryptophan analogs into proteins has proven to be relatively simple compared to other synthetic amino acid probes.[6,7] The azatryptophan analogs can be incorporated into proteins by expressing the protein in an *E. coli* tryptophan auxotroph while replacing the azatryptophan analogs for natural tryptophan in the growth media. An integrated approach has been established that allows domain specific incorporation of azatryptophan analogs using the auxotroph followed by expressed protein ligation.[25] Both 7-azatryptophan and 6-azatryptophan have been successfully incorporated into proteins and peptides with very promising results.[7,25–26] Two other azatryptophan analogs, 4-azatryptophan and 5-azatryptophan, may also be useful as probes for protein dynamics and structure.

Indole is the chromophoric moiety of tryptophan and the photophysics of indole are explored to avoid complications of the zwitterionic form of tryptophan in experimental studies.[3] Therefore, the azaindole isomers are studied in this work to avoid the complications associated with the azatryptophan isomers. The four azaindole isomers of interest, 4-azaindole (4AI), 5-azaindole (5AI), 6-azaindole (6AI) and 7-azaindole (7AI), are shown in Fig. 1. The picture in Fig. 2 shows the fluorescence of the four different azaindole isomers (10 mM aqueous solution) when irradiated with UV light (254 nm). Visually, the

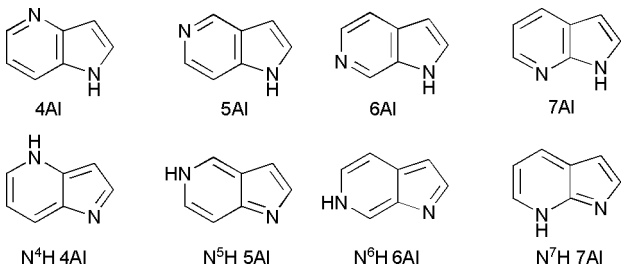

Fig. 1 Azaindole isomers and tautomers explored in this work.

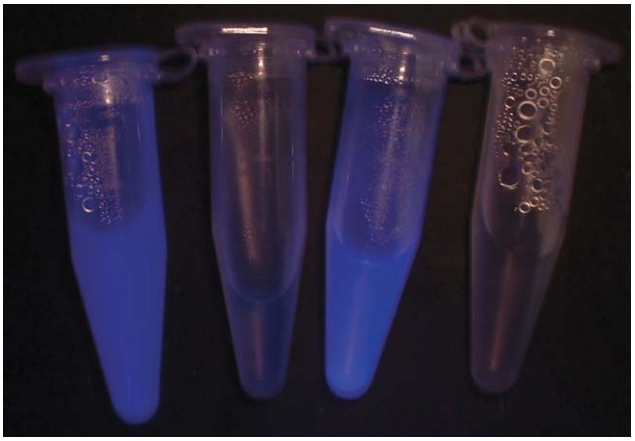

Fig. 2 A 10 mM solution of each azaindole isomer under a UV lamp ($\lambda = 254$ nm). From left to right: 4AI, 5AI, 6AI, and 7AI.

DOI:10.1039/b506652b

fluorescence intensity of 4AI and 6AI are significantly greater than the other isomers, which makes 4AI and 6AI of additional interest.

Another interesting property of the azaindole isomers is their ability to undergo excited state tautomerization, which has been demonstrated with 7AI and 6AI. Excited state tautomerization of 7AI has been thoroughly explored. There are two established mechanisms for the tautomerization of 7AI, an excited state double proton exchange (Fig. 3a) and cyclic intermediate involving one water molecule (Fig. 3b).[9,10] Recently, it was shown that 6AI also undergoes excited state tautomerization evident by the presence of a fluorescent band at 440 nm in strong base and methanol–water mixtures. The tautomerism of 6AI was proposed to occur by protonation at N^6 in the excited state, followed by deprotonation at N^1 also in the excited state.[7]

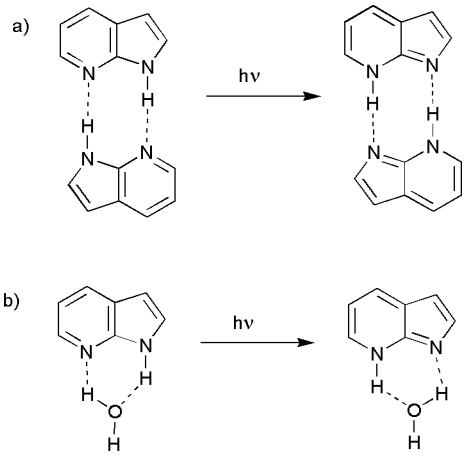

Fig. 3 (a) Excited state double proton transfer of 7-azaindole; (b) excited state proton transfer with one water molecule.

Indole is the base structure of a number of very important biological molecules. The azaindole isomers could also be useful for other applications besides peptide and protein dynamics. 7AI is currently being explored as a molecular probe for use in auxin physiology; 7AI is the chromophoric moiety of 7-azaindole-3-acetic acid.[24] Considering the great potential for its use as a fluorescent probe, we are interested in characterizing the fluorescence properties of 4AI and 5AI. The ability of the azaindole isomers to tautomerize in solution is an important aspect regarding the fluorescence, because each tautomer has a unique fluorescent spectrum. Through experimental and computational methods, we determined the ground state and excited state characteristics of each azaindole isomer and the potential for excited state tautomerization of 4AI and 5AI. In addition, we computed the effects of solvation on the energy differences of each azaindole isomer.

Theoretical and experimental

A. Computations

The ground state studies of the azaindole isomers in both gas phase and solvent were done using density functional theory. All stationary structures were characterized as minima by computation of second derivatives of the energy (no imaginary frequencies). We employed Becke's three parameter exchange functional,[11] and the Lee–Yang–Parr nonlocal correlation functional in conjuction with a B3LYP/6–31+G** basis set implemented in Gaussian 94.[12] Nucleus independent chemical shifts (NICS), a measure of aromaticity,[23] were computed using density functional theory as well.

Bulk solvent effects were included with self consistent reaction field (SCRF) computations using the isodensity polarized continuum model (IPCM).[13] The IPCM model was chosen because the effects of solvation are incorporated into the iterative SCF computation, which results in a proper variational condition. The dielectrics of the three solvents mimic chloroform (4.8), methanol (32.7) and water (78.4) at 298 K.

Both time dependent DFT[27] (TDDFT) and *ab initio* methods were used for the excited state transition energies. The *ab initio* method chosen is the configuration interaction with single excitations (CIS) procedure.[14] CIS was used to obtain the optimized excited state energies and geometries. The same basis set was used (6–31+G**) as for the DFT computations. TDDFT computations utilized Gaussian 98[16] while all other computations were carried out using Gaussian 94.[15]

B. Synthesis of 4AI (Scheme 1)

Two routes were explored for obtaining 2-methyl-3-nitropyridine from 2-chloro-3-nitropyridine.

Method 1. *Diethyl-2-(3-nitropyridyl)malonate (**2**).* 2-Chloro-3-nitropyridine (2.0 g, 12.5 mmol) was added to 0.3 g (12.5 mmol) NaH in 10 mL of dry DMF with stirring under nitrogen. Diethyl malonate (2.0 g, 12.5 mmol) was added dropwise, resulting in a brownish-red mixture. After the reaction was allowed to stir for 1 h, the solvent was evaporated giving a brown oil. The oil was diluted with 50 mL of water, followed by neutralization with a few drops of acetic acid. The precipitate was extracted with dichloromethane three times, and the combined organic layers were dried with $MgSO_4$. The solvent was removed and the remaining oil was then passed over a silica column and eluted with a 30% ethyl acetate in hexanes. The product diethyl-2-(3-nitropyridyl)malonate (1.8 g) was isolated as yellow crystals (50% yield). All analytical data agree with previously reported synthesis.[17]

*2-Methyl-3-nitropyridine (**3**).* Diethyl-2-(3-nitropyridyl)-malonate (1.0 g, 3.9 mmol) was dissolved in 50 mL of 6 N HCl and refluxed for 8 h. The solvent was evaporated leaving a brownish oil that solidified upon cooling. 50 mL of saturated sodium carbonate was added, and the solution was extracted three times with 25 mL of dichloromethane. The organic layers

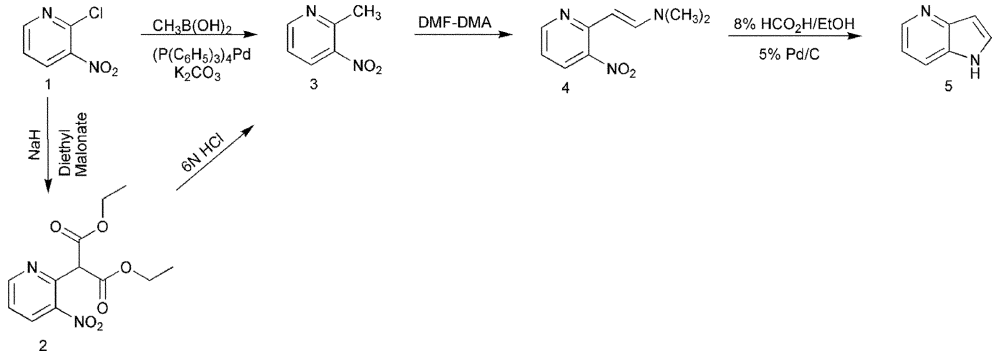

Scheme 1

were combined and dried with $MgSO_4$ followed by removal of solvent yielding 0.42 g of 2-methyl-3-nitropyridine as a brown solid (86% yield). All analytical data agree with previously reported synthesis.[17]

Method 2. *2-Methyl-3-nitropyridine (**3**).* A mixture of (0.16 g, 1 mmol) 2-chloro-3-nitropyridine, tetrakis(triphenylphosphine)Pd (0.12 g, 0.1 mmol), methylboronic acid (0.07 g, 1.1 mmol) and potassium carbonate (0.4 g, 3 mmol) was added to dioxane and refluxed for 2 d. The solvent was evaporated and the mixture was separated on a silica column using an ethyl acetate–hexanes solvent. 2-methyl-3-nitropyridine (0.06 g) was obtained as a light brown solid (43% yield). All analytical data agree with previously reported synthesis.[18]

*Preparation of the enamine (**4**).* 2-Methyl-3-nitropyridine (0.5 g, 3.6 mmol) was dissolved in 10 mL of dry DMF and stirred under nitrogen. DMF–DMA (0.86 g, 7.2 mmol) was added dropwise. The reaction was heated to 90 °C. After 15 min of heating, a deep reddish color began to appear, and it was allowed to react for 4 h. After 4 h, the solvent was removed by evaporation. The red oil obtained (0.65 g) was used without further purification. All analytical data agree with previously reported synthesis.[17]

*4-azaindole (**5**).* The crude enamine (0.65 g, 3.4 mmol) was dissolved in 10 mL of 8.8% formic acid in methanol. The mixture was added dropwise to a flask containing 10 mL of 8.8% formic acid in methanol with 0.2 g of 5% Pd/C, stirred under nitrogen. The reaction proceeded for 4 h, until the red color had completely disappeared. The Pd catalyst was removed by filtration through celite, and the filtrate was then concentrated. After sitting overnight, the product, 4AI, crystallized (0.12 g). The crystallized product was filtered and washed with hexanes. The filtrate was then evaporated to dryness, and the remaining solid was recrystallized with ethyl acetate and hexanes to give a combined yield of 0.31 g (78%). All analytical data agree with previously reported synthesis.[17]

C. Synthesis of 5AI

5AI was synthesized as previously described.[17]

D. General procedure for the synthesis of the *N*-methyl-azaindole isomers (Scheme 2)[19]

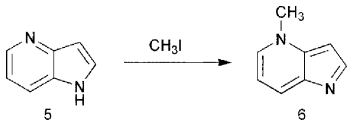

Scheme 2

The azaindole isomer (100 mg, 0.85 mmol) was dissolved in 2 mL dry DMF. Iodomethane (120 mg, 0.85 mmol) was added to the mixture, and the reaction was allowed to stir for 3 h. The solvent was evaporated, leaving a brown oil. The remaining brown oil was dissolved in 25 mL dichloromethane and extracted three times with 15 mL of saturated sodium carbonate. The organic layer was dried with $MgSO_4$ followed by evaporation and the mixture was then loaded onto an alumina column. The parent azaindole was eluted first with chloroform. The *N*-methyl azaindole was eluted with 20% ethanol–chloroform to give approximately 20 mg of each azaindole isomer (18% yield).[19]

Absorbance and fluorescence spectroscopy

The absorbance spectra were obtained on a Cary 1E UV/Vis spectrophotometer. The fluorescence experiments were obtained on a Fluorolog Spectrofluorimeter by Instruments S.A., Inc. The path length was 1 cm and all experiments were performed at 20 °C. Each of the azaindole isomers was analyzed in water and 1 M NaOH solution. The excitation wavelength for 4AI was 293 nm and 270 nm for 5AI. The excitation wavelengths were also computed as described above for comparison.

Table 1 Energy differences between tautomers. (energy of N^n–H-energy of N^1–H) at B3LYP/6–31+G**

Isomer	Ground state/kcal mol^{-1}	Excited state/kcal mol^{-1}
4AI	11.6	−15.5
5AI	11.4	−17.6
6AI	10.1	−14.0
7AI	12.5	−18.1

Results and discussion

Many theoretical and experimental studies have been reported on 7AI including its tautomerization. It has been well established that the N^1–H tautomer of both 7AI and 6AI is the most stable tautomer in the ground state.[6,7,10,20,21] Rasmussen and Mahadevan reported that all four azaindole isomers are more stable in the N^1–H tautomeric form based on *ab initio* computations using the minimal STO-3G basis set at the HF level of theory, not taking into account effects of electron correlation.[19] In Table 1 we summarize the results of computing the ground states of the tautomers of the azaindole isomers B3LYP/6–31+G**. The N^1–H tautomer is more stable by more than 10 kcal mol^{-1} for each of the azaindole isomers; the N^1–H tautomer has often been referred to as the "normal" tautomer for this reason.[6] Among the normal tautomers, 6AI is the lowest in energy while 7AI is the highest, with 2.4 kcal mol^{-1} separating the two. On the other hand, in the excited state the other tautomer (referred to as N^n–H, where $n = 4$, 5, 6 or 7 depending on the azaindole isomer) is more stable, by at least 15 kcal mol^{-1}. Previous experimental work agrees with the computations, as both 7AI and 6AI do tautomerize in the excited state, provided that the solvent conditions are suitable (*i.e.*, alkaline solution or combination of water with a less polar co-solvent).[6,7]

The following investigation was to see if 5AI and 4AI also tautomerize in the excited state. Computations indicate that the N^n–H tautomers are more stable by at least 15 kcal mol^{-1} in the excited state and therefore, the possibility of tautomerization is likely. However, due to the geometric arrangement of the pyridine and pyrrole nitrogens of 4AI and 5AI, the mechanism of tautomerization will differ from that of 7AI (Fig. 3). The mechanism of tautomerization would be similar to 6AI, a proposed mechanism being excitation of the normal tautomer, followed by solvent proton abstraction at N^6 in the excited state, and the deprotonation of N^1 also in the excited state.[7]

The relative energies of the N^1–H azaindole isomers are listed in Table 2. The values are reported relative to 4AI. 7AI is lower in energy by approximately 4 kcal mol^{-1} in the ground state compared to other N^1–H azaindole isomers. 4AI, 5AI and 6AI all have nearly the same ground state energy as the N^1–H tautomer. Likewise, in the excited state, 7AI is again the lower in energy by as much as 9.4 kcal mol^{-1} in the N^1–H tautomer.

The relative energies of the N^n–H tautomers are summarized in Table 2. N^5–H 5AI is more stable by about 5 kcal mol^{-1} in the ground state compared to other N^n–H azaindole isomers. N^4–H

Table 2 Energies of azaindole isomers relative to 4AI at B3LYP/6–31+G**

Isomer	Ground state/kcal mol^{-1}	Excited state/kcal mol^{-1}
4AI	0.0	0.0
5AI	−0.3	1.0
6AI	0.4	2.8
7AI	−4.4	−6.6
N^4H 4AI	0.0	0.0
N^5H 5AI	−1.4	−1.1
N^6H 6AI	−1.0	4.4
N^7H 7AI	3.6	−9.2

4AI and N^6–H 6AI have nearly the same ground state energy as N^5–H 5AI, while N^7–H 7AI is highest in energy However, in the excited state, N^7–H 7AI is the lowest in energy by as much as 13.6 kcal mol^{-1}.

Spectroscopic studies

The fluorescence spectra of 5AI and 4AI were measured to determine if these isomers tautomerize in the excited state and to characterize the fluorescence wavelength of the tautomer and the protonated species. The N^4-methyl and N^5-methyl derivatives were synthesized to help characterize the fluorescence spectra, since the presence of a methyl group locks the azaindole into the N^n–H tautomeric form. As seen from the spectra in Fig. 4 and 5, at high pH (*i.e.*, pH = 14), 4AI and 5AI both tautomerize. In the case of 4AI, we see the presence of two bands, one at 390 nm and another at 480 nm. The N^4-methyl-4AI fluorescence spectrum shows a single band at 480 nm in the presence of 1 M NaOH. The band at 480 nm is assigned to the N^4–H 4AI tautomer based on the fluorescence spectrum of N^4-methyl-4AI. The fluorescence spectrum of 5AI in 1 M NaOH shows only one broad band with a maximum at 455 nm. N^5-methyl-5AI has a virtually identical fluorescence spectrum with a maximum at 460 nm. The fluorescent band at 455 nm is assigned to the N^5–H 5AI tautomer. For comparison, the spectra of 5AI and 4AI in water are shown. These fluorescent bands are the protonated form of the azaindole isomer. The protonated 4AI has a maximum at 415 nm, and the protonated 5AI has a maximum at 410 nm. Table 3 summarizes the fluorescence data for each of the azaindole isomers.

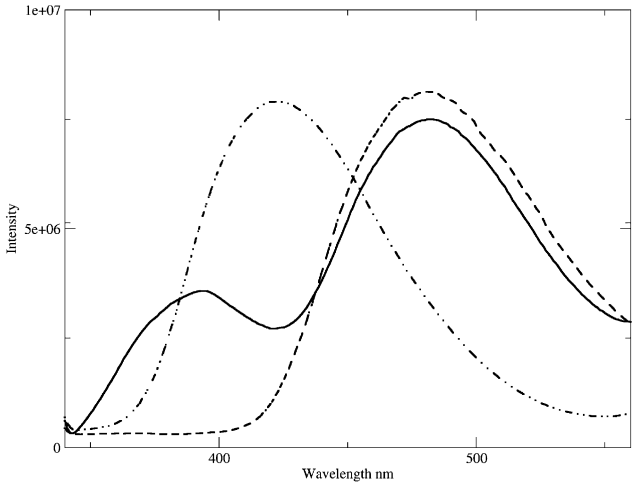

Fig. 4 Normalized fluorescence spectra of 4AI in H_2O (dot-dash line), 1 M NaOH (solid line) and N^4-Methyl-4AI in 1 M NaOH (dashed line).

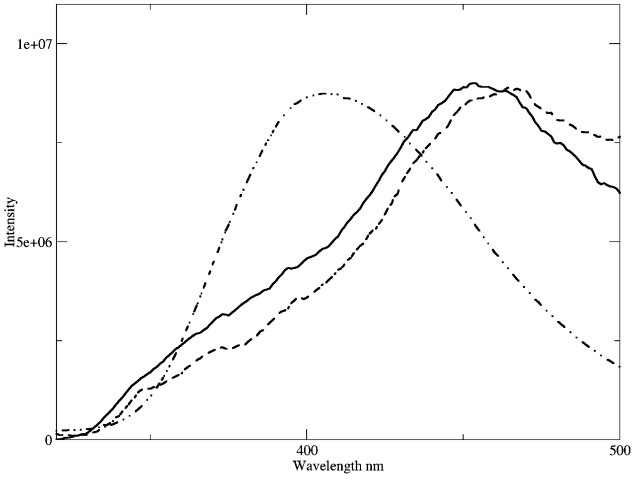

Fig. 5 Normalized fluorescence spectra of 5AI in H_2O (dot-dash line), 1 M NaOH (solid line) and N^5-Methyl-*5AI in 1 M NaOH (dashed line).

Table 3 Fluorescence maxima of the tautomers and protonated azaindole isomers. Both 6AI and 7AI fluorescence maxima taken from the specified reference

Isomer	Wavelength/nm
4AI	N/A
4AI–H^+	415
N^4H 4AI	480
5AI	N/A
5AI–H^+	410
N^5H 5AI	450
6AI	350[a]
6AI–H^+	380[a]
N^6H 6AI	440[a]
7AI	385[b]
7AI–H^+	440[b]
N^7H 7AI	500[b]

[a] Values from ref. 7. [b] Values from ref. 6.

Table 4 Computed and experimental absorbance wavelengths

Isomer	Experimental[a]	CIS	TDDFT
4AI	293	242	270
N^4H 4AI	370	336	383
5AI	270	248	260
N^5H 5AI	310	358	355
6AI	300	240	264
N^4H 6AI	355	318	345
7AI	296	251	271
N^7H 7AI	350	373	387

[a] Values taken from ref. 19.

We explored the excitation energies using two different methods. First, we used time-dependent DFT, which computes a vertical excitation from the optimized ground state.[22] In order to estimate the effect of adiabatic transistions, the optimized excited state geometries and energies were computed using the CI Singles method; TD-DFT optimizations can currently not yet be performed. The computed and experimental excitation wavelength and excited state energies are listed in Table 4. The experimental wavelengths were taken from ref. 19 Across the board, TD-DFT vertical (without geometry optimization) absorptions were closer to experiment than those from optimized excited state geometries at the CIS level of theory. This is easily understandable as electronic absorption phenomena are vertical in nature. With the exception of N^5–H 5AI and 6AI, all TDDFT excitation wavelengths were within 25 nm of the experimental values. The computed and experimental values listed in Table 4 both indicate a significant excitation energy difference between the N^1–H and N^n–H tautomers. The difference arises from the lower energy of the N^1–H species relative to the N^n–H tautomer in the ground state. However, in the excited state, the N^n–H tautomer is lower in energy relative to the N^1–H tautomer (Table 1). As expected, the greater difference in the HOMO–LUMO energy gap is reflected in the higher excitation energy observed in the N^1–H azaindole tautomer.

Solvent effects

The energy of each azaindole tautomer in the presence of a continuous solvent dielectric was explored to determine the effects of a solvent dielectric on the tautomer energy differences. All the azaindole isomers were stabilized by the dielectric constant of the solvent, but the largest decrease in the energy difference between tautomers occurred for 5AI and 6AI as seen in Fig. 6 and Table 5. The energy difference of both isomers was decreased by 5.8 and 4.8 kcal mol^{-1}, respectively. The energy

Table 5 Energy differences between tautomers in the presence of different dielectrics

Isomer	Gas phase	Chloroform	Methanol	Water
4AI	11.6	9.1	8.3	8.2
5AI	11.4	7.4	5.8	5.6
6AI	10.1	6.7	5.5	5.3
7AI	12.5	10.0	9.1	9.0

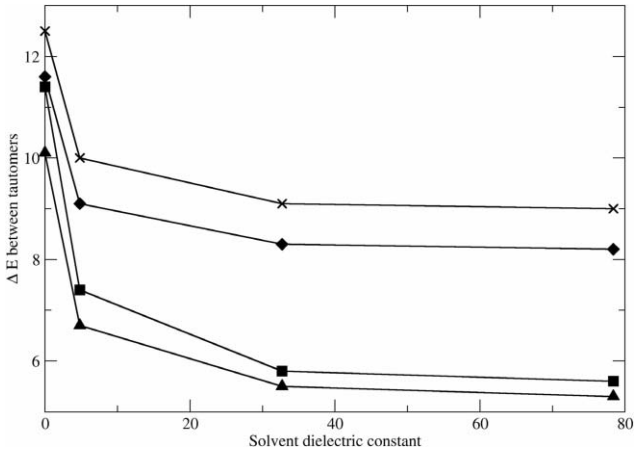

Fig. 6 Energy differences between tautomers in the presence of a continuous solvent dielectric; × = 7AI, ▲ = 6AI, ■ = 5AI, ◆ = 4-azaindole.

difference of 4AI and 7AI tautomers decreased by 3.4 and 3.5 kcal mol^{-1}, respectively.

The effect of solvation was greater on the N^n–H tautomer than on the N^1–H tautomer as shown in Table 6. The introduction of a solvent dielectric constant induces an increase in the dipole of the molecule, which occurs to a greater extent on the N^n–H tautomer. As the solvent dielectric increases, a linear increase in the dipole of each isomer is observed. Since each of the N^n–H isomers has a higher dipole moment than the N^1–H tautomers, the solvation energy of that tautomer is greater. The higher solvation energy of the N^n–H tautomer results in the lower energy difference between the tautomers. Table 6 shows the solvation stabilization energies of each isomer and their tautomer by the water dielectric. Clearly, each of the N^n–H isomers has a greater solvation stabilization energy than the corresponding N^1–H tautomer. The greatest solvation stabilization energy was observed for the N^5–H 5AI and the N^6–H 6AI isomers, while the solvation energy of the corresponding N^1–H tautomers are nearly the same, which explains the decreased energy difference shown in Fig. 5.

Gordon and co-workers suggested that part of the reason for the greater stability of the N^1–H tautomer over the N^7–H tautomer of 7AI is due to aromatic stabilization of the N^1–H tautomer.[21] In the N^7–H tautomer, the pyrrole portion has an exocyclic π bond, similar to fulvene, which is considered to be non-aromatic (Fig. 7). Schleyer and co-workers have

Table 6 Energy differences from gas phase to solvent dielectric equal to water (78.4) at B3LYP/6–31+G**

Isomer	Solvation stabilization energy/kcal mol^{-1}
4AI	8.1
N^{4}H 4AI	11.5
5AI	8.3
N^{5}H 5AI	14.2
6AI	8.0
N^{4}H 6AI	12.8
7AI	6.5
N^{7}H 7AI	9.9

Table 7 NICS(1) values at B3LYP/6–31+G**

Molecule	Pyridine ring	Pyrrole ring
4AI	−10.6	−10.1
N^{4}H 4AI	−9.1	−12.9
5AI	−10.8	−10.3
N^{5}H 5AI	−9.1	−13.2
6AI	−10.9	−10.5
N^{4}H 6AI	−8.6	−13.4
7AI	−10.6	−10.2
N^{7}H 7AI	−9.4	−12.5
Benzene	−10.2	—

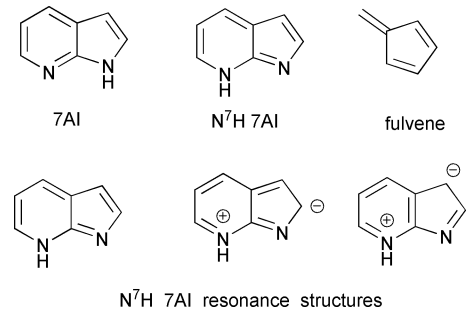

Fig. 7 Structure comparisons of 7AI, N^7-7AI and fulvene.

shown that computing the chemical shielding at the center of an aromatic ring can provide a qualititative measurement of the aromaticity of the ring.[23] These types of computations have been given the term NICS, nucleus independent chemical shieldings. NICS were computed 1 Å above the center (NICS(1)) of both the pyrrole and pyridine rings for each of the azaindole isomers (Table 7).[23] Interestingly, a NICS(1) computation of each ring shows that both the N^1–H tautomer and the N^n–H tautomer are almost equally *aromatic*. In fact, the pyrrole ring of the N^n–H tautomer is even more aromatic than the N^1–H tautomer although the resonance structure suggests an exocyclic π bond. The NICS(1) value of −10.2 for benzene was included as a reference point. This can be rationalized by dipolar resonance structures that avoid the fulvene-type double bond configuration and allow for complete cyclic, and hence aromatic, delocalization (Fig. 7).

Conclusions

Both 4AI and 5AI display excited state tautomerization in the presence of strong base demonstrated by the fluorescence spectra in comparison with the N^n–CH$_3$ analogs. The protonated form of 4AI has an emission maximum at 415 nm and the N^4–H tautomer has a fluorescence maximum at 480 nm. The protonated form of 5AI has an emission maximum at 410 nm and the N^5–H tautomer has a fluorescence maximum at 450 nm. All the azaindole isomers are more stable in the N^1–H tautomer by at least 10 kcal mol^{-1} in the ground state. In the excited state, all the N^n–H tautomers are lower in energy. The polarity of the solvent helps to reduce the energy difference between the tautomer in the ground state by as much as 5.8 kcal mol^{-1}, but not enough to reverse the ground state tautomer preference. The preference for the N^1–H tautomer appears to not be due to aromatic stabilization considering both tautomers are equally aromatic.

Acknowledgements

This work was supported by the National Science Foundation (PRS, CHE-0209857) and the National Institute of Health (RSP, GM-42588).

References

1 A. Clayton and W. Sawyer, *Euro. Biophys. J.*, 2002, **31**, 9.
2 C. Royer, *Biophys J.*, 1993, **65**, 9.
3 J. Lakowicz, *Photochem. Photobiol.*, 2000, **72**, 421.
4 Y. Engelborghs, *Spectrochim. Acta, Part A*, 2001, **57**, 2255.
5 D. Creed, *Photochem. Photobiol.*, 1984, **39**, 537–562.
6 A. Smirnov, D. English, R. Rich, J. Lane, L. Teyton, A. Schwabacher, S. Luo, R. Thornburg and J. Petrich, *J. Phys. Chem. B*, 1997, **101**, 2758.
7 S. Twine, L. Murphy, R. Phillips, P. Callis, M. Cash and A. Szabo, *J. Phys. Chem. B*, 2003, **107**, 637.
8 Q. Li, H. Du and H. Hu, *Biopolymers*, 2003, **72**, 116.
9 C. Chang and T. Lin, *Huaxue*, 1997, **55**, 83.
10 J. Catalan and M. Kasha, *J. Phys. Chem. A*, 2000, **104**, 10812.
11 A. Becke, *J. Chem. Phys.*, 1993, **98**, 5648.
12 C. Lee, W. Yang and E. Parr, *Phys. Rev. B*, 1988, **37**, 785.
13 C. Curutchet, C. J. Cramer, D. G. Truhlar, M. F. Ruiz-Lopez, D. Rinaldi, M. Orozco and F. J. Luque, *J. Comput. Chem.*, 2003, **24**, 284.
14 J. Foresman, M. Head-Gordon, J. Pople and M. Frisch, *J. Phys. Chem.*, 1992, **96**, 135.
15 M. J. Frisch, G. W. Trucks, H. B. Schlegel, P. M. W. Gill, B. G. Johnson, M. A. Robb, J. R. Cheeseman, T. Keith, G. A. Petersson, J. A. Montgomery, K. Raghavachari, M. A. Al-Laham, V. G. Zakrzewski, J. V. Ortiz, J. B. Foresman, J. Cioslowski, B. B. Stefanov, A. Nanayakkara, M. Challacombe, C. Y. Peng, P. Y. Ayala, W. Chen, M. W. Wong, J. L. Andres, E. S. Replogle, R. Gomperts, R. L. Martin, D. J. Fox, J. S. Binkley, D. J. Defrees, J. Baker, J. P. Stewart, M. Head-Gordon, C. Gonzalez, and J. A. Pople, *GAUSSIAN 94*, Gaussian, Inc., Pittsburgh, PA, 1995.
16 M. J. Frisch, G. W. Trucks, H. B. Schlegel, G. E. Scuseria, M. A. Robb, J. R. Cheeseman, V. G. Zakrzewski, J. A. Montgomery, Jr., R. E. Stratmann, J. C. Burant, S. Dapprich, J. M. Millam, A. D. Daniels, K. N. Kudin, M. C. Strain, O. Farkas, J. Tomasi, V. Barone, M. Cossi, R. Cammi, B. Mennucci, C. Pomelli, C. Adamo, S. Clifford, J. Ochterski, G. A. Petersson, P. Y. Ayala, Q. Cui, K. Morokuma, D. K. Malick, A. D. Rabuck, K. Raghavachari, J. B. Foresman, J. Cioslowski, J. V. Ortiz, A. G. Baboul, B. B. Stefanov, G. Liu, A. Liashenko, P. Piskorz, I. Komaromi, R. Gomperts, R. L. Martin, D. J. Fox, T. Keith, M. A. Al-Laham, C. Y. Peng, A. Nanayakkara, C. Gonzalez, M. Challacombe, P. M. W. Gill, B. G. Johnson, W. Chen, M. W. Wong, J. L. Andres, M. Head-Gordon, E. S. Replogle and J. A. Pople, *GAUSSIAN 98 (Revision A.9)*, Gaussian, Inc., Pittsburgh, PA, 1998.
17 M. Sloan and R. Phillips, *Bioorg. Med. Chem. Lett.*, 1992, **2**, 1053.
18 C. Niu, J. Li, T. Doyle and S. Chen, *Tetrahedron*, 1998, **54**, 6311.
19 I. Mahadevan and M. Rasmussen, *Tetrahedron*, 1993, **49**, 7337.
20 M. Gordon, *J. Phys. Chem.*, 1996, **100**, 3974.
21 G. Chaban and M. Gordon, *J. Phys. Chem. A*, 1999, **103**, 185.
22 C. Jamorski Jodicke and H. P. Lüthi, *J. Am. Chem. Soc.*, 2003, **125**, 252.
23 P. v. R. Schleyer, M. Manoharan, Z. Wang, B. Kiran, H. Jiao, R. Puchta and N. van Eikema Hommes, *J. Org. Lett.*, 2001, **3**, 2465.
24 S. Antolic, B. Kojic-Prodic and V. Magnus, *Acta Crystallogr., Sect. C*, 2000, **56**, 1026.
25 V. Muralidharan, J. Cho, M. Trester-Zedlitz, L. Kowalik, B. Chait, D. Raleigh and T. Muir, *J. Am. Chem. Soc.*, 2004, **126**, 14004.
26 V. De Filippis, S. De Boni, E. De Dea, D. Dalzoppo, C. Grandi and A. Fontana, *Protein Sci.*, 2004, **13**, 1489.
27 M. Petersilka, U. J. Gossmann and E. K. U. Gross, *Phys. Rev. Lett.*, 1996, **76**, 1212.